Temporal Leakage in Analysis of Electromagnetic Systems

Antonije R. Djordjević[1], Dejan V. Tošić[1], Alenka G. Zajić[2], Marija M. Nikolić[1], Dragan I. Olćan[1], and Izabela D. Jovanović[3]

[1]School of Electrical Engineering
University of Belgrade
King Alexander's Boulevard 73, 11120 Belgrade, Serbia
Tel: +381 11 3218 329; Fax: +381 11 3248 681; E-mails: edjordja@etf.rs; tosic@etf.rs; mnikolic@etf.rs; olcan@etf.rs

[2]School of Computer Science
Georgia Institute of Technology
266 Ferst Dr, Atlanta, GA 30332-0765, USA
Tel: +1 404 385-6604; E-mail: azajic@cc.gatech.edu

[3] Telekom Srbija
Katićeva 14, 11000 Belgrade, Serbia
Tel: +381 11 3069 723; Fax: +381 11 3628 015; E-mail izabela@telekom.rs

Abstract

Temporal leakage occurs when the time-domain response of a linear electromagnetic system is computed from frequency-domain data using the inverse discrete Fourier transform. Although the temporal leakage occurs in most practical cases, this phenomenon is not recognized in the literature covering electromagnetics, antennas, and microwaves. The purpose of the paper is to demonstrate and explain the temporal leakage.

Keywords: Discrete Fourier transform; computational electromagnetics; time-domain response; temporal leakage

1. Introduction

Various linear time-invariant electromagnetic systems are most conveniently analyzed in the frequency domain because there exist mature computational techniques (e.g., [1]) and related software (e.g., [2, 3]). Most measurements of antennas and microwave systems are also performed in the frequency domain (using vector network analyzers), yielding a discrete set of frequency-domain data. In order to obtain the time-domain response of such systems, the inverse discrete Fourier transform (inverse DFT) is often used (e.g., [4]), which is implemented as a fast Fourier transform (FFT) algorithm. In the application of the discrete Fourier transform, an apparently noncausal response can be obtained in the time domain, in spite of careful modeling in the frequency domain or carefully calibrated measurements. This unexpected response appears in the form of fast oscillations that occur before a sharp edge of the physically meaningful time-domain response.

The same problem also occurs in the analysis of electrical circuits. An example is shown in Figure 7 of [5], where the noncausal oscillations are mistakenly attributed to the Gibbs phenomenon. However, the problem is actually associated with an inherent feature of the discrete Fourier transform that is referred to as the "temporal leakage" [6-11]. This phenomenon is mentioned only in very few references away from the electromagnetic community, although its counterpart, the "spectral leakage," is extensively elaborated in the literature (e.g., [12, 13]).

The purpose of this paper is to show some typical cases where temporal leakage occurs in electromagnetic analysis and measurements, and to give a mathematical explanation of the phenomenon. Consequently, in Section 2, the discrete Fourier transform is briefly revisited. In Section 3, the mathematical background of temporal leakage is elaborated. In Section 4, several examples are given illustrating this phenomenon.

 ISSN 1045-9243/2012/$26 ©2012 IEEE

2. Discrete Fourier Transform

The discrete Fourier transform can be introduced by considering a periodic sequence of equally spaced Dirac delta functions (impulses) in the time domain, $\delta(t)$, and *exactly* evaluating the corresponding Fourier transform, which is also a periodic sequence of equally spaced impulses. The proof is given below. This approach is somewhat unusual, but it is useful for explaining temporal leakage and some other peculiarities of the discrete Fourier transform.

Consider a sequence of N impulses in the time domain (temporal functions), at time instants $0, \Delta t, 2\Delta t, ..., (N-1)\Delta t$, where Δt is the time step and $N\Delta t = T$. The amplitudes of the impulses are $x_0, x_1, ..., x_{N-1}$. This sequence is periodically repeated with a period T. Mathematically, this sequence can be defined on the interval $0 \le t < T$ as

$$x_{\delta T}(t) = \sum_{n=0}^{N-1} x_n \delta(t - n\Delta t). \tag{1}$$

It is then periodically repeated using $x_\delta(t + lT) = x_{\delta T}(t)$, where l is an arbitrary integer. Alternatively, we can write

$$x_\delta(t) = \sum_{n=-\infty}^{+\infty} x_n \delta(t - n\Delta t), \quad x_{n+lN} = x_n. \tag{2}$$

The sequence $x_\delta(t)$ can also be represented in terms of the comb function, as follows. The comb function is a periodic train of impulses with a period T:

$$\Delta_T(t) = \sum_{m=-\infty}^{+\infty} \delta(t - mT). \tag{3}$$

The function $x_\delta(t)$ can be expressed as a sum of interleaved comb functions, which are shifted for $n\Delta t$, $n = 0, ..., N-1$:

$$x_\delta(t) = \sum_{n=0}^{N-1} x_n \Delta_T(t - n\Delta t), \tag{4}$$

where each comb function is multiplied (weighted) by x_n.

We now evaluate the Fourier transform (Fourier integral) of $x_\delta(t)$. Since $\Delta_T(t)$ is a periodic function, it can be expanded in a Fourier series. The coefficients of the series are

$$c_k = \frac{1}{T} \int_{-T/2}^{T/2} \delta(t) \mathrm{e}^{-\frac{2\pi jkt}{T}} \, \mathrm{d}t = \frac{1}{T},$$

where k is an integer, $k \in (-\infty, +\infty)$, and j is the imaginary unit, so that $\Delta_T(t) = \frac{1}{T} \sum_{k=-\infty}^{+\infty} \mathrm{e}^{\frac{2\pi jkt}{T}}$. On the other hand, the Fourier transform of $\mathrm{e}^{\frac{2\pi jkt}{T}}$ is $\delta\left(f - \frac{k}{T}\right)$. Hence, the Fourier transform of $\Delta_T(t)$ is

$$\begin{aligned} \frac{1}{T} \sum_{k=-\infty}^{+\infty} \delta\left(f - \frac{k}{T}\right) &= \Delta f \sum_{k=-\infty}^{+\infty} \delta(f - k\Delta f) \\ &= \Delta f \Delta_{\Delta f}(f), \end{aligned} \tag{5}$$

where $\Delta f = \frac{1}{T}$. It is also a comb of delta functions, but in the spectral (frequency) domain, with the spectral-domain period Δf.

The Fourier transform of each comb function in Equation (4) can be obtained from Equation (5) by using the shift theorem, i.e., it is given by

$$\begin{aligned} \Delta f \Delta_{\Delta f}(f) \mathrm{e}^{-2\pi jfn\Delta t} &= \Delta f \sum_{k=-\infty}^{+\infty} \delta(f - k\Delta f) \mathrm{e}^{-2\pi jfn\Delta t} \\ &= \Delta f \sum_{n=-\infty}^{+\infty} \delta(f - k\Delta f) \mathrm{e}^{-2\pi j\frac{kn}{N}}. \end{aligned}$$

This is because $\delta(f)g(f) = \delta(f)g(0)$, where $g(f)$ is an arbitrary function defined at $f = 0$ and continuous at $f = 0$, and because $\mathrm{e}^{-2\pi jk\Delta fn\Delta t} = \mathrm{e}^{-2\pi j\frac{kn}{N}}$, because $\Delta t \Delta f = \frac{1}{N}$.

By summing the Fourier transforms for all comb functions, a sequence of weighted delta functions in the spectral domain is obtained. Each delta function is thereby multiplied by

$$X_k = \frac{1}{T} \sum_{n=0}^{N-1} x_n \mathrm{e}^{-2\pi j\frac{kn}{N}} = \Delta f \sum_{n=0}^{N-1} x_n \mathrm{e}^{-2\pi j\frac{kn}{N}}, \quad k \in (-\infty, +\infty).$$

Since n is an integer, we have $\mathrm{e}^{-2\pi j\frac{(k+N)n}{N}} = \mathrm{e}^{-2\pi j\frac{kn}{N}}$, so that X_k is a periodic sequence of complex numbers, with a basic period N. It is hence sufficient to consider X_k only on the basic period, i.e., for $k = 0, ..., N-1$, in the same way as it is sufficient to consider x_n only for $n = 0, 1, ..., N-1$.

Following a similar derivation, we can show that

$$x_n = \Delta t \Delta f \sum_{k=0}^{N-1} X_k \mathrm{e}^{2\pi j\frac{nk}{N}} = \frac{1}{N} \sum_{k=0}^{N-1} X_k \mathrm{e}^{2\pi j\frac{nk}{N}}.$$

We have hence obtained formulas for the physical (de-

normalized) discrete Fourier transform (DFT) and the corresponding inverse discrete Fourier transform (IDFT):

$$X_k = \Delta f \sum_{n=0}^{N-1} x_n \mathrm{e}^{-2\pi j \frac{kn}{N}}, \quad k = 0, 1, ..., N-1, \qquad (6)$$

$$x_n = \frac{1}{N} \sum_{k=0}^{N-1} X_k \mathrm{e}^{2\pi j \frac{nk}{N}}, \quad n = 0, 1, ..., N-1. \qquad (7)$$

These transforms relate the amplitudes of a periodic sequence of impulses in the time domain (x_n) to the amplitudes of a periodic sequence of impulses in the frequency domain (X_k). Note that the relations in Equations (6) and (7) are *exact*, and that the sequences of pulses in both domains are infinite and periodic.

The normalized form of the discrete Fourier transform is obtained by artificially taking $\Delta f = 1$ (also neglecting the units), so that

$$X_k = \sum_{n=0}^{N-1} x_n \mathrm{e}^{-2\pi j \frac{kn}{N}}, \quad k = 0, 1, ..., N-1, \qquad (8)$$

whereas the formula for the normalized inverse discrete Fourier transform is identical to Equation (7). The normalized forms are practically the only ones found in the literature, and the available FFT algorithms are based on Equations (7) and (8). From now on in this paper, we consider only the normalized forms.

If Equation (1) represents a physical time-domain signal, then the amplitudes $x_0, x_1, ..., x_{N-1}$ are real numbers. The corresponding spectrum has a conjugate symmetry. Hence, the infinite sequence of complex numbers $\{X_k\}$ has a conjugate symmetry: $X_{-k} = X_k^*$ for any integer *k*. Assuming *N* to be even, due to the periodicity of $\{X_k\}$ this sequence on the basic period looks like the following:

$$\{X_0, X_1, \ldots, X_{N/2-1}, X_{N/2}, X_{N/2+1}, \ldots, X_{N-1}\} = \{X_0, X_1, \ldots, X_{N/2-1}, X_{N/2}, X_{N/2-1}^*, \ldots, X_1^*\}. \qquad (9)$$

The terms $X_{N/2}$ and X_0 are purely real, due to the conjugate symmetry of $\{X_k\}$. If *N* is odd, the middle (purely real) term in this sequence does not exist, but X_0 is still purely real.

When analyzing or measuring an electromagnetic system in the frequency domain and evaluating the time-domain response using the inverse discrete Fourier transform, one should hence properly define the sequence $\{X_k\}$ in Equation (7) in order to obtain real-valued elements of the sequence $\{x_n\}$. The first part of $\{X_k\}$ is taken from the computed or measured data, and the second part is defined based on the conjugate symmetry, as in Equation (9).

In practice, the basic application of the normalized discrete Fourier transform is to *approximately* evaluate the spectrum of a real, continuous-time, non-periodic signal $x(t)$. The signal $x(t)$ might be an electric field, voltage, current, etc. In numerical applications, we can only deal with the values of the signal at a finite number of discrete time instants.
This application of the discrete Fourier transform can be introduced in two ways. One way is to deal with the samples of the original continuous-time signal, and the other way is to replace the original signal by a discrete-time signal. In both cases, we assume that the signal is almost time-limited to the interval $t \in [0, T)$.

Following the first approach, we take the samples (signal values) at *N* equally spaced time instants, $t_n = n\Delta t$, $n = 0, 1, ..., N-1$, i.e., we take $x_n = x(n\Delta t)$. We approximate the Fourier integral of $x(t)$ by a sum of "rectangles," i.e.,

$$\int_{-\infty}^{+\infty} x(t) \mathrm{e}^{-2\pi jft} \mathrm{d}t \approx \int_0^T x(t) \mathrm{e}^{-2\pi jft} \mathrm{d}t \approx \sum_{n=0}^{N-1} x(n\Delta t) \mathrm{e}^{-2\pi jfn\Delta t} \Delta t.$$

We further assume that the spectrum of $x(t)$, $X(f)$, is almost frequency limited to the interval $f \in \left[0, \frac{N}{2T}\right)$, and we consider this spectrum only at discrete frequencies $f_k = k\Delta f = \frac{k}{T}$, $k = 0, 1, ..., N/2-1$ (for *N* even). Knowing that the spectrum has a conjugate symmetry, we thus effectively consider *N* discrete values of the spectrum. Since $f_k n\Delta t = \frac{nk}{N}$, we obtain $X(k\Delta f) \approx \Delta t \sum_{n=0}^{N-1} x(n\Delta t) \mathrm{e}^{-2\pi j \frac{kn}{N}}$. This sum is the normalized discrete Fourier transform, so that $X(k\Delta f) \approx \Delta t X_k$. Note that to obtain a proper approximation of the spectrum, we need to perform the multiplication by Δt.
Using the normalized inverse discrete Fourier transform, we obtain the values x_n in a similar way, as $x(n\Delta t) \approx \Delta f \sum_{k=0}^{N-1} X_k \mathrm{e}^{2\pi j \frac{nk}{N}}$. Hence, $x(n\Delta t) \approx N\Delta f x_n$. Note that $N\Delta t\Delta f = 1$, so that this product is absorbed into the sequences of the direct and inverse discrete Fourier transforms.

Some FFT algorithms use identical formulas for the direct and inverse FFT, apart from a sign change in the exponent. In such cases, the inverse discrete Fourier transform does not include the division by *N*, so that $x(n\Delta t) \approx \Delta f x_n$.

Assuming that N is even, the spectral components $X_0, X_1, ..., X_{N/2-1}$ approximate the values of the spectrum $X(f)$ of the signal $x(t)$ at a set of discrete frequencies, i.e.,

$$X_k = \frac{1}{\Delta t} X(k\Delta f), \quad n = 0, 1, ..., N/2-1 .$$

According to the second approach to using the discrete Fourier transform to approximately evaluate the spectrum of the signal $x(t)$, we replace the continuous-time signal, $x(t)$, by the discrete-time signal, $x_{dt}(t) = x_{\delta T}(t)\Delta t$, where $x_{\delta T}(t)$ is given by Equation (1). The need for multiplication by Δt can be justified in two ways. First, the unit for the delta function, $\delta(t)$, is s^{-1}, so that we have to restore the original unit for the signal, $x(t)$. Second, we want $x(t)$ and $x_{dt}(t)$ to have approximately identical spectra, so that $x(t)$ and $x_{dt}(t)$ should have practically equal integrals over any interval the length of which is Δt (note that $\int_{-\varepsilon}^{\varepsilon} \delta(t)\,\mathrm{d}t = 1$ for any $\varepsilon > 0$). Following this approach, upon evaluating the Fourier integral, we again obtain the spectral samples to be $X(k\Delta f) \approx \Delta t X_k$.

In conclusion to this section, we point out that the discrete Fourier transform is an *exact* transform that maps a periodic sequence of impulses in the temporal domain into a periodic sequence of impulses in the spectral domain. However, when used to analyze a continuous-time signal (or a function the temporal samples of which are known), the discrete Fourier transform only *approximately* evaluates spectral samples of such a signal. Similarly, the inverse discrete Fourier transform only approximately evaluates temporal samples of a function the spectral samples of which are known. We thereby perform discretization both in the time domain and in the frequency domain. By applying the discrete Fourier transform, we hence *always* introduce an aliasing error, because a continuous-time function cannot be limited both in the time domain and in the frequency domain. However, if we know that the function under consideration is *practically* limited to the time interval $(0, t_{max})$ and also *practically* limited to the frequency range $(0, f_{max})$, the application of the discrete Fourier transform/inverse discrete Fourier transform yields useful results.

Care should also be taken when applying the discrete Fourier transform to the analysis of high-frequency electromagnetic problems, which always involve a delay. If the delay exceeds the period *T*, and/or if the response does not settle down to zero fast enough, the response from one time window will penetrate into the subsequent time window, which will appear as a wraparound of the response. A particular example where this periodicity causes trouble is the evaluation of the step response (the response to the Heaviside function). When applying the discrete Fourier transform, the Heaviside function must be replaced by a rectangular pulse that which jumps from 0 to 1 at the beginning of the time window, and returns to zero around the middle of the same time window. The duration of the time window must be sufficient to allow the response to practically vanish within this window.

3. Temporal Leakage

The simplest yet illustrative case where one can get acquainted with temporal leakage is a delay line. Such a line can be a model of an ideal matched transmission line. If the line is excited by an impulse located at $t = 0$, i.e., by $\delta(t)$, and if the delay is τ, the signal at the output of the line is given by $\delta(t-\tau)$. The objective is to evaluate this response using the normalized discrete Fourier transform. Since it is assumed that the impulse is located at $t = 0$, we have $x_0 = 1$, $x_n = 0$, $n = 1, ..., N-1$. We assume that $0 < \tau < (N-1)\Delta t$. Applying Equation (8) yields the frequency-domain samples, $X_k = 1$, $k = 0, 1, ..., N-1$. The delay is next expressed as $\tau = p\Delta t$ ($0 < p < N-1$), and this delay is simulated in the spectral domain by multiplying X_k by $\exp(-2\pi jkp/N)$, $k = 0, ..., N/2-1$. (This simulation mimics the analysis of an electromagnetic system or a circuit in the frequency domain.) The sample $X_{N/2}$ is peculiar, because it must remain purely real. Hence, $X_{N/2}$ is multiplied only by $\mathrm{Re}\{\exp(-\pi jp)\}$. The remaining samples, for $k = N/2+1, ..., N-1$, are filled according to Equation (9). Thereafter, the inverse normalized discrete Fourier transform, Equation (7), is applied.

If p is an integer, a clean response is obtained using *MATLAB* [14], as shown in Figure 1, for $p = 150$. If this is not the case (e.g., $p = 300.5$), the response contains oscillations (temporal leakage).

The temporal leakage can be explained by analytically evaluating the sum in Equation (7). Due to the conjugate symmetry in the spectral domain, one can write

$$x_n = \frac{1}{N}\left\{1 + 2\,\mathrm{Re}\left(\sum_{k=1}^{\frac{N}{2}-1} \mathrm{e}^{-\frac{2\pi j}{N}kp}\,\mathrm{e}^{\frac{2\pi j}{N}kn}\right) + \mathrm{Re}\left[\mathrm{e}^{\pi j(n-p)}\right]\right\}. \tag{10}$$

After summing the series in Equation (10) and some manipulations given in the Appendix, the result becomes

$$x_n = \frac{1}{N}\frac{\sin N\pi\alpha}{\tan \pi\alpha}, \tag{11}$$

where $\alpha = \dfrac{n-p}{N}$. Considering x_n as a function of α, it has a global maximum for $\alpha = 0$. This maximum is 1.

However, p is an arbitrary given constant, whereas n is

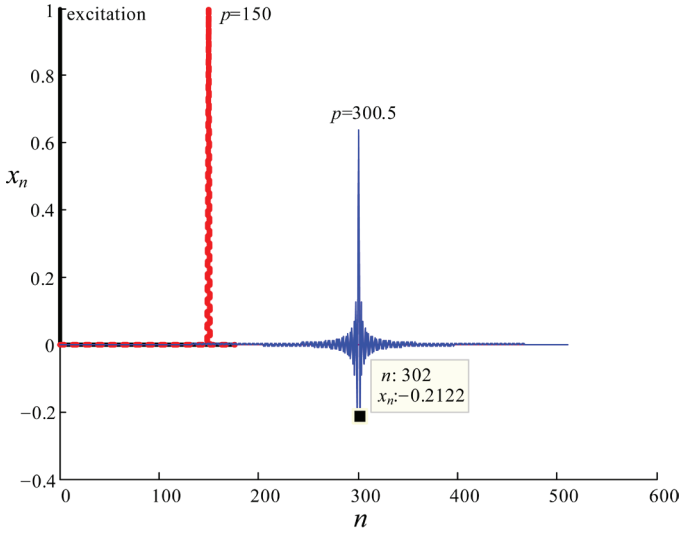

Figure 1. The impulse excitation of a delay line and the computed response (for $N=512$) when $p=150$ and $p=300.5$.

an integer. Hence, the global maximum can be attained only if p is also an integer, when the maximum occurs for $n=p$ ($x_p=1$). In that case, all other samples are $x_n=0$, $n=0,\ldots,N-1, n\neq p$, and a clean response is obtained, which is an impulse delayed for $\tau=p\Delta t$ after the excitation. If p is not an integer, temporal leakage occurs. When $\alpha \ll 1$, i.e., in the vicinity of the delayed impulse, $\tan\pi\alpha \approx \pi\alpha$, so that

$$x_n \approx \frac{\sin N\pi\alpha}{N\pi\alpha} = \frac{\sin\pi(n-p)}{\pi(n-p)} = \operatorname{sinc}(n-p). \quad (12)$$

The largest sample is the one for which the index n is closest to p, but now $x_n<1$. The largest leakage occurs if $p=m+0.5$, where m is an integer. In that case, there are two largest samples, the values of which are approximately $\frac{2}{\pi}\approx 0.6366$. They are surrounded by two negative samples, the values of which are approximately $-\frac{2}{3\pi}\approx -0.2122$, which can be verified in Figure 1.

Temporal leakage can also be explained in the following way. Let us consider the sequence in Equation (7). If we want to delay this sequence for τ, all spectral components X_k, $k\in(-\infty,+\infty)$, must be multiplied by $\exp(-2\pi jf\tau)$. This multiplication modifies only the phase of X_k (Figure 2) by reducing it by $2\pi f\tau$, which is plotted with the line denoted "natural." However, in the general case, the resulting spectral components do not form a periodic sequence any more.

When we apply the discrete Fourier transform to evaluate the delay, we modify the phases of only the samples for $k=0,\ldots,N-1$, which belong to the basic spectral interval. (In Figure 2, it is assumed that $N=8$.) This phase shift is denoted as the "discrete Fourier transform basic interval." Thereafter, we periodically repeat the samples from this basic interval. Consequently, the phase shift is periodically repeated as denoted in Figure 2 by the "discrete Fourier transform periodically repeated." Note that the phase shift of the samples for $k=-N/2+1,\ldots,0,\ldots,N/2-1$ coincides with the natural phase shift.

Modifying the phase shift by an integer multiple of 2π does not change anything. Hence, we can try to overlap the discrete Fourier transform phase shift with the natural phase shift. (In the example shown in Figure 2, the attempted shift was 2π, viz. -2π.) In the general case, the overlapping will not be possible and phase jumps would occur, as illustrated in Figure 2. These jumps are the sources of the temporal leakage.

The only exceptions are cases when the natural phase shift at the sample N is an integer multiple of 2π (i.e., when the delay, τ, is an integer multiple of Δt). In that case, the result obtained using the discrete Fourier transform exhibits a perfect delay. An example is the natural delay labeled "perfect" in Figure 2.

4. Examples

As the first example in this section, Figure 3 shows the response of a delay line to a rectangular pulse with a width of $50\Delta t$. Temporal leakage occurs around the pulse's edges if the delay is not an integer multiple of Δt. In the response for $p=300.5$, interference occurred between the ringing gener-

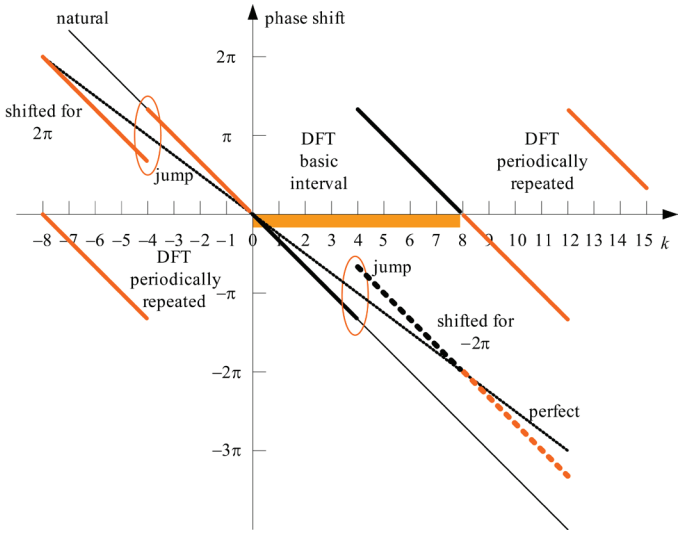

Figure 2. An illustration of the phase shifting when using the discrete Fourier transform that causes temporal leakage.

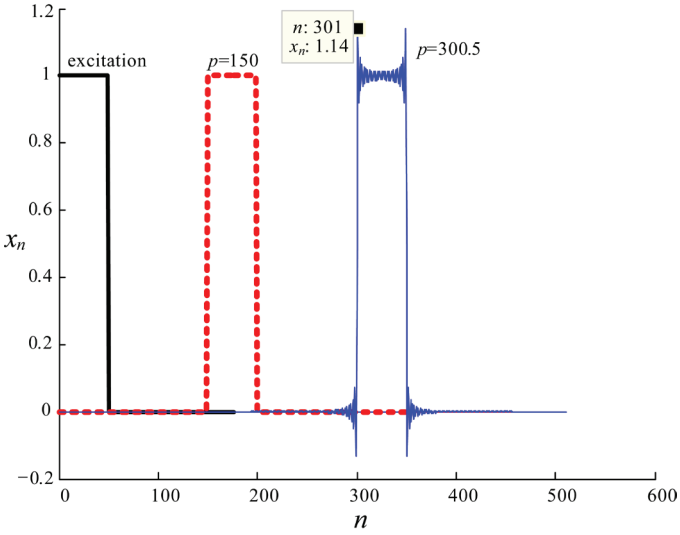

Figure 3. Rectangular-pulse excitation of a delay line and the computed response (for $N = 512$) when $p = 150$ and $p = 300.5$.

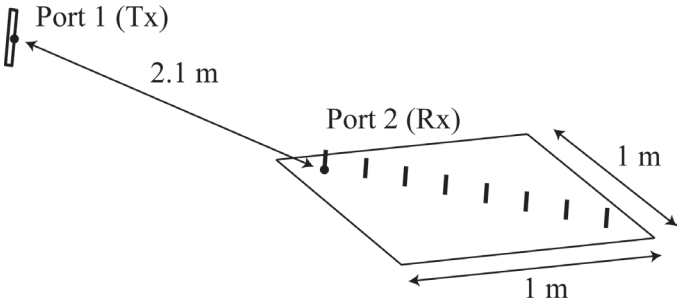

Figure 4. The system analyzed, with two antennas 2.1 m apart.

ated at the two transients, due to a small pulse width. If the pulse was sufficiently wide, the interference would be negligible. The maximum overshoots and undershoots occurred when $p \approx m + 0.4$ or $p \approx m + 0.6$, and they amounted to about 14% of the edge's height. Note that the oscillations associated with the Gibbs phenomenon are given in terms of the sine-integral function [15]. The resulting undershoots and overshoots at the transients would be about 9% of the edge height, i.e., smaller than those associated with the worst-case temporal leakage. The temporal leakage and the Gibbs phenomena look similar, but they have different causes. Temporal leakage arises due to the discretization of a continuous signal, while the Gibb's effect arises due to limiting the bandwidth of the signal.

As the next example, we considered two wire antennas, separated by a distance of 2.1 m. The measured and simulated structure consisted of a 225 mm-long folded dipole, which acted as a transmitting antenna (Tx), and eight 80 mm-long monopoles placed along the diagonal of a 1 m × 1 m aluminum plate (Figure 4). The first dipole acted as the receiving antenna (Rx), while the other seven monopoles were terminated in 50 Ω loads [16]. The response was obtained by calculating the scattering parameter S_{21} using *WIPL-D* [3], and by measuring S_{21} (in the frequency domain) using a vector network analyzer and performing the inverse discrete Fourier transform. Figure 5a shows the impulse response. The noncausal ringing caused by the temporal leakage (for $t < 7.1$ ns) was significantly reduced if the separation between the antennas was increased by just 25 mm (Figure 5b), since this increase accidentally introduced a proper additional time delay and the corresponding phase shift.

Finally, Figure 6a shows the measured and simulated step responses of a differential-mode fast digital-signal link. The

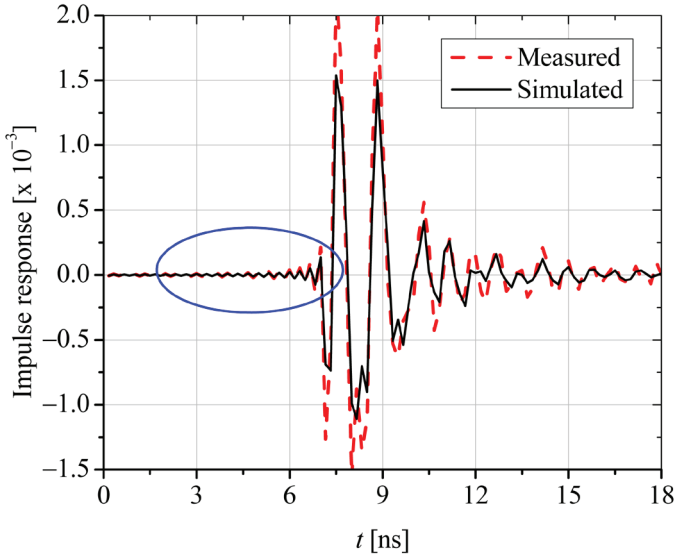

Figure 5a. The impulse response of the two antennas shown in Figure 4.

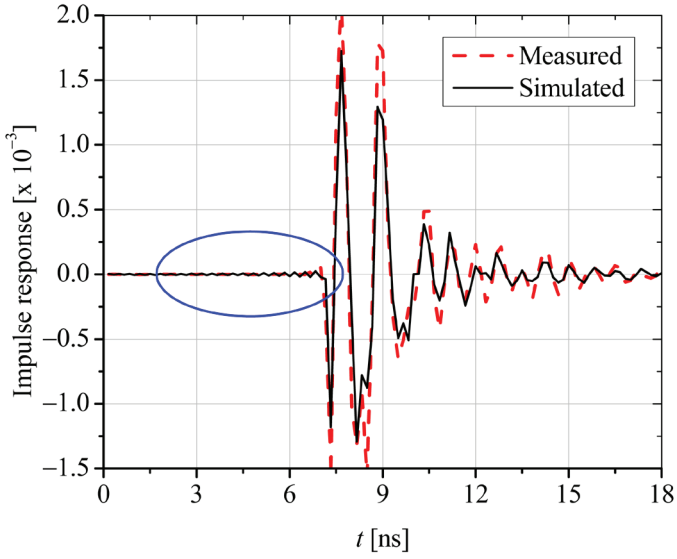

Figure 5b. The impulse response of the two antennas shown in Figure 4 when the distance between the antennas was increased by 25 mm.

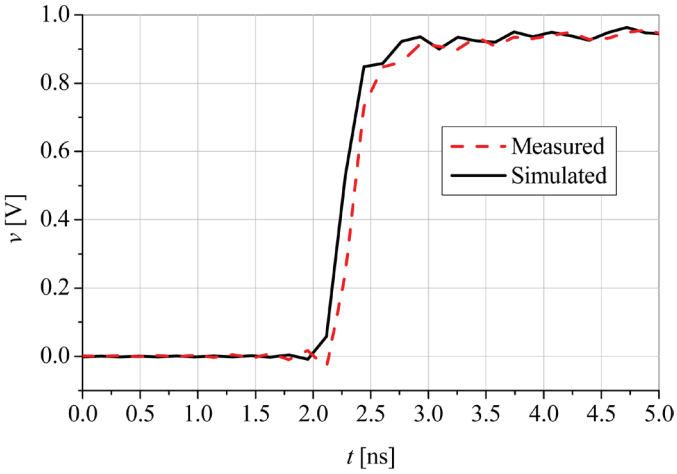

Figure 6a. The step response of a fast digital-signal link.

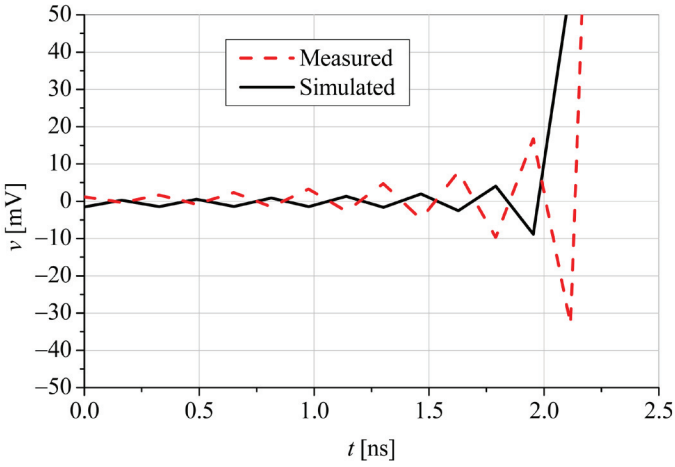

Figure 6b. An enlarged version of a portion of Figure 6a, showing the ringing due to temporal leakage.

link encompassed three multilayer printed-circuit boards and corresponding connectors. The simulated response was computed in the frequency domain using a model of the dielectric parameters [17] along with a model of the per-unit-length resistance and inductance [18] that guaranteed a causal response. The latter model included the edge effects, the proximity effects, the skin effects, and the effects of surface roughness. The model of the link also included discontinuities at the connectors. The impulse response was first evaluated using the inverse discrete Fourier transform of the scattering parameter S_{21} (involving frequency samples up to about 3 GHz), followed by a convolution to obtain the step response. Even after the convolution (which introduced smoothing), oscillations due to temporal leakage persisted in the response (Figure 6b). The period of the oscillations equaled twice the time step used in computations. The oscillations were clearly visible before the propagated step occurred. Thereafter, they were blended with oscillations due to multiple reflections on the link.

With the above examples, we have demonstrated that temporal leakage appears in results of numerical simulations and in measurements using vector network analyzers (which is true both if the analyzer has a built-in time-domain option, and if the inverse discrete Fourier transform of the scattering parameters is externally performed).

The effects of temporal leakage are artifacts in the time-domain response that occur around fast transitions of the response. The artifacts are quasi-oscillatory, their period equals twice the time step, and their amplitudes decay slowly away from the transitions. The oscillations occur not only after a transition, but also prior to it, so that an apparently non-causal response of a causal system is obtained.

In the worst-case scenario, the maximum effect of the temporal leakage can be as high as 21% of the impulse response (Figure 1), and 14% of the step response or the pulse response (Figure 3), for low-loss wideband systems (such as a simple transmission line). However, in other practical cases, the effect of the temporal leakage is usually smaller (Figures 5 and 6), depending on the bandwidth of the system and the spectrum of the time-domain excitation.

Temporal leakage is less pronounced in systems with dispersion (e.g., a lossy transmission line) because sharp transitions cannot occur in such cases. Furthermore, temporal leakage can be kept low by appropriately shaping the excitation functions, e.g., by applying a Gaussian pulse, which is often used to find figures of merit for time-domain radiators [19, 20]. In such cases, the amplitudes of the oscillations due to temporal leakage are on the order of a few percent or even less of the actual response, so that the temporal leakage is often blended with oscillations due to other causes. However, note that in some cases, the impulse response is indispensable (e.g., when evaluating responses by convolution and when modeling nonlinear systems [21]), when the response to the Dirac delta function cannot be replaced by the response to the Gaussian pulse.

Temporal leakage can be practically eliminated in a system the response of which is affected by a single physical time delay (e.g., a single-path transmission between two matched antennas). In such a case, the number of frequencies and/or the frequency step at which the response is measured or computed may be changed, with the aim of making this delay equal to an integer multiple of the time step. For example, we can freeze the frequency step and change the upper frequency used in the computations by changing the total number of samples. A peculiarity of this procedure is that temporal leakage will periodically decrease and increase as the number of samples is changed. However, in the general case – i.e., when the system is characterized by two or more non-commensurate time delays (e.g., a multipath transmission between two antennas, or a microwave circuit with several reflection points) – temporal leakage will always be present.

5. Conclusions

This paper explained and demonstrated temporal leakage. First, we mathematically explained why temporal leakage occurs. We also showed that when applying the discrete Fourier transform, an apparently noncausal response can be obtained in the time domain in spite of careful modeling in the frequency domain. Finally, we presented some typical cases where temporal leakage occurs in electromagnetic analysis, as well as in measurements.

6. Acknowledgments

The authors thank their student, Mr. Djordje Mirković, for providing motivation for the paper and meticulous reading.
This work was supported in part by the Serbian Ministry of Education and Science under Grant TR32005, and by COST action IC1102 VISTA.

7. References

1. B. M. Kolundžija and A. R. Djordjević, *Electromagnetic Modeling of Composite Metallic and Dielectric Structures*, Norwood, MA, Artech House, 2002.

2. HFSS 13.0, ANSYS, Inc., *3D Full-wave Electromagnetic Field Simulation*, http://www.ansoft.com/products/hf/hfss/.

3. WIPL-D Pro 8.0, 3D Electromagnetic Solver, http://www.wipl-d.com.

4. D. I. Olćan, M. M. Nikolić, B. M. Kolundžija, and A. R. Djordjević, "Time-Domain Response of 3-D Structures Calculated Using WIPL-D," Proceedings of ACES 2007, Verona, Italy, March 2007, pp. 525-531.

5. M. M. Potrebić, D. V. Tošić, and P. V. Pejović, "Understanding Computation of Impulse Response in Microwave Software Tools," *IEEE Transactions on Education*, **EDU-53**, 4, November 2010, pp. 547-555.

6. M. S. O'Brien and S. M. Kramer, "Temporal Leakage and Its Effects on Resolution in Deconvolution of Ultrasonic Signals," Review of Progress in Quantitative Nondestructive Evaluation, **11A,** Proceedings of 18th Annual Review, Brunswick, ME, July 28-August 2, 1991, pp. 911-918.

7. P. M. A. Warwick, *Analysis and Application of the Spectral Warping Transform to Digital Signal Processing*, Thesis, Institute of Information Sciences and Technology, Massey University, Palmerston North, New Zealand, 2007.

8. M. R. Coble, G. C. Papen, and C. S. Gardner, "Computing Two-Dimensional Unambiguous Horizontal Wavenumber Spectra from OH Airglow Images," *IEEE Transactions on Geoscience and Remote Sensing*, **36**, 2, March 1998, pp. 368-382.

9. G. Yao and S.-I Chu, "Strong Field Effects in Above-Threshold Detachment of a Model Negative Ion," *Journal of Physics B: Atomic Molecular and Optical Physics*, **25**, 2, January 1992, pp. 363-376.

10. S. Zegenhagen, A. Werner, A. Weller, and T. Klinger, "Analysis of Alfvén Eigenmodes in Stellarators Using non-Evenly Spaced Probes," *Plasma Physics and Controlled Fusion*, **48**, pp. 1333-1346, 2006.

11. J. D. Cameron, *Stall Inception in a High-Speed Axial Compressor*, PhD dissertation, University of Notre Dame, Indiana, USA, 2007.

12. W. Y. Yang, T. G. Chang, I. H. Song, Y. S. Cho, J. Heo, W. G. Jeon, J. W. Lee, and J. K. Kim, *Signals and Systems with MATLAB*, Heidelberg, Springer, 2009.

13. D. Havelock, S. Kuwano, and M. Vorländer, *Handbook of Signal Processing in Acoustics, Volume 1*, New York, Springer, 2008.

14. MATLAB, The MathWorks, Inc., http:// www.mathworks.com/.

15. D. W. Kammler, *A First Course in Fourier Analysis*, New York, Cambridge University Press, 2007, pp. 44-45.

16. M. M. Nikolić, A. Nehorai, and A. R. Djordjević, "Biologically Inspired Sensing on UAV Platform," 2011 IEEE International Symposium on Antennas and Propagation and USNC-URSI Meeting *Digest*, July 3-8, 2011, Spokane, WA, USA, pp. 1537-1540.

17. A. R. Djordjević, R. M. Biljić, V. D. Likar-Smiljanić, and T. K. Sarkar, "Wideband Frequency-Domain Characterization of FR-4 and Time-Domain Causality," *IEEE Transactions on Electromagnetic Compatibility*, **EMC-43**, 4, November 2001, pp. 662-667.

18. I. Jovanović, *Ultrafast Digital-Signal Interconnects on Printed-Circuit Boards*, MSc thesis, University of Belgrade, School of Electrical Engineering, Belgrade, Serbia, 2010.

19. C. E. Baum, E. G. Farr, and D. V. Giri, "Review of Impulse-Radiating Antennas," in W. R. Stone (ed.), *Review of Radio Science 1996-1999*, Oxford, Oxford University Press, 1999, Chapter 16, pp. 403-438.

20. D. Ghosh, A. De, M. C. Taylor, T. Sarkar, C. Wicks, and E. L. Mokole, "Transmission and Reception by Ultra-Wideband (UWB) Antennas," *IEEE Antennas and Propagation Magazine*, **48**, 5, October. 2006, pp. 67-99.

21. A. R. Djordjević and T. K. Sarkar, "Transient Analysis of Electromagnetic Systems with Multiple Lumped Nonlinear

Loads," *IEEE Transactions on Antennas and Propagation*, **AP-33**, 5, May 1985, pp. 533-539.

8. Appendix

We derive here Equation (11). We start from Equation (10), and sum the geometric series as

$$\sum_{k=1}^{\frac{N}{2}-1} \mathrm{e}^{-\frac{2\pi j}{N}kp}\,\mathrm{e}^{\frac{2\pi j}{N}kn} = \mathrm{e}^{\frac{2\pi j}{N}(n-p)}\,\frac{\mathrm{e}^{\frac{2\pi j}{N}\left(\frac{N}{2}-1\right)(n-p)}-1}{\mathrm{e}^{\frac{2\pi j}{N}(n-p)}-1}.$$

We extract from the numerator the term $\mathrm{e}^{\frac{\pi j}{N}\left(\frac{N}{2}-1\right)(n-p)}$, leaving

$$\mathrm{e}^{\frac{\pi j}{N}\left(\frac{N}{2}-1\right)(n-p)} - \mathrm{e}^{-\frac{\pi j}{N}\left(\frac{N}{2}-1\right)(n-p)} = 2j\sin\left(\frac{N}{2}-1\right)\frac{\pi(n-p)}{N}.$$

Similarly, from the denominator we extract the term $\mathrm{e}^{\frac{\pi j}{N}(n-p)}$, leaving

$$\mathrm{e}^{\frac{\pi j}{N}(n-p)} - \mathrm{e}^{-\frac{\pi j}{N}(n-p)} = 2j\sin\frac{\pi(n-p)}{N}.$$

The sum thus becomes

$$\sum_{k=1}^{\frac{N}{2}-1} \mathrm{e}^{-\frac{2\pi j}{N}kp}\,\mathrm{e}^{\frac{2\pi j}{N}kn} = \mathrm{e}^{\frac{\pi j}{2}(n-p)}\,\frac{\sin\left(\frac{N}{2}-1\right)\frac{\pi(n-p)}{N}}{\sin\frac{\pi(n-p)}{N}}.$$

Substituting this sum into Equation (10) and setting $\frac{n-p}{N}=\alpha$ yields

$$x_n = \frac{1}{N}\left[1+2\cos\frac{N}{2}\pi\alpha\,\frac{\sin\left(\frac{N}{2}-1\right)\pi\alpha}{\sin\pi\alpha}+\cos N\pi\alpha\right].$$

Finally, using the trigonometric identities

$$1+\cos N\pi\alpha = 2\cos^2\frac{N\pi\alpha}{2}$$

and

$$\sin\left(\frac{N}{2}-1\right)\pi\alpha = \sin\frac{N}{2}\pi\alpha\,\cos\pi\alpha - \cos\frac{N}{2}\pi\alpha\,\sin\pi\alpha,$$

Equation (11) is obtained.

Introducing the Feature Article Authors

Antonije R. Djordjević was born in Belgrade, Serbia, in 1952. He received the BSc, MSc, and PhD from the School of Electrical Engineering, University of Belgrade, in 1975, 1977, and 1979, respectively. In 1975, he joined the School of Electrical Engineering, University of Belgrade, as a Teaching Assistant. He was promoted to Assistant Professor, Associate Professor, and Professor, in 1982, 1988, and 1993, respectively. In 1983, he was a Visiting Associate Professor at Rochester Institute of Technology, Rochester, NY. Since 1992, he has been an Adjunct Scholar with Syracuse University, Syracuse, NY. In 1997, he became a Corresponding Member of the Serbian Academy of Sciences and Arts, and he became a full member in 2006. His main area of interest is numerical electromagnetics, in particular applied to fast digital signal interconnects, wire and surface antennas, microwave passive circuits, and electromagnetic compatibility problems.

Dejan V. Tošić was born in Belgrade, Serbia, in 1957. He received the BSc (1980), MSc (1986), and PhD (1996) from the School of Electrical Engineering, University of Belgrade, Serbia. He is currently a full Professor with the School of Electrical Engineering, University of Belgrade. He is a coauthor of the book *Filter Design for Signal Processing Using MATLAB and Mathematica* (Prentice-Hall, 2001, translated into Chinese by PHEI, Beijing, China, 2004), a coauthor of the book *WIPL-D Microwave: Circuit and 3D EM Simulation for RF & Microwave Applications* (Artech House, 2005), and a coauthor of *SchematicSolver*, a software package for symbolic and numerical analysis, processing, and design of analog and digital systems (http://www.wolfram.com/ products/applications/ schematicsolver/). His research interests include symbolic computation and signal processing, RF and microwave filter design, and the design of passive microwave circuits.

Alenka G. Zajić received her BSc and MSc from the School of Electrical Engineering, University of Belgrade, in 2001 and 2003, respectively. She received her PhD in Electrical and Computer Engineering from the Georgia Institute of Technology in 2008. In 2010, she joined the School of Computer Science, Georgia Institute of Technology, where she is a Visiting Assistant Professor. Her research interests are in wireless communications and applied electromagnetics. Dr. Zajić received the Best Paper Award at ICT 2008, the Best Student Paper Award at WCNC 2007, and was also the recipient of the Dan Noble Fellowship in 2004, awarded by Motorola Inc. and the IEEE Vehicular Technology Society for quality impact in the area of vehicular technology.

Dragan I. Olćan is an Assistant Professor in the School of Electrical Engineering, University of Belgrade, Serbia, where he received his BSc, MSc, and PhD in 2001, 2004, and 2008, respectively. He is a coauthor of two commercial electromagnetic software codes, five journal papers, about forty conference papers, and four university textbooks. His main research interests are the diakoptic approach to numerical electromagnetic analysis, optimization algorithms applied to electromagnetic design, time-domain electromagnetic analysis, and applied electromagnetics.

Marija M. Nikolić received the BSc, MSc, and PhD from the University of Belgrade in 2000, 2003, and 2007, respectively. In 2001, she joined the School of Electrical Engineering, University of Belgrade, as a Teaching Assistant. In 2008, she was promoted to Assistant Professor. In 2011, she obtained the PhD in Electrical Engineering from Washington University in St. Louis, USA. She is interested in inverse scattering, array processing, and antenna analysis and design.

Izabela D. Jovanović was born in Belgrade, Serbia, in 1972. She received her BSc and MSc degrees from the School of Electrical Engineering, University of Belgrade, in 1998 and 2010, respectively. From 1998 until 2004, she worked as an R&D engineer at the Institute for Microwave Techniques and Electronics (IMTEL) in Belgrade. Since 2004, she has been with "Telekom Srbija" in Belgrade as a leading engineer.